Flexure of the India plate underneath the Bhutan Himalaya

Paul Hammer,[1] Théo Berthet,[2] György Hetényi,[3,1] Rodolphe Cattin,[2] Dowchu Drukpa,[4] Jamyang Chophel,[4] Sarah Lechmann,[1] Nicolas Le Moigne,[2] Cédric Champollion,[2] and Erik Doerflinger[2]

Received 19 June 2013; revised 18 July 2013; accepted 22 July 2013; published 23 August 2013.

[1] We investigate flexural geometry and rheology of the India plate beneath the eastern Himalaya from a new gravity data set acquired in Bhutan. Compared to the well-studied Nepal Himalaya, the obtained Bouguer anomaly profiles across the range show shorter wavelength flexure of the lithosphere with a narrower and shallower foreland basin. This new data set and seismic Moho constraints are interpreted together in terms of lithospheric flexure using a 2-D thermomechanical model. Our results suggest that the strongest layer of the continental lithosphere beneath Bhutan is the upper mantle, as it is beneath Nepal. The observed west-to-east decrease in flexural wavelength is associated with weakening mantle rheology. The simulations show that this decrease can be related to ductile mantle behavior: either hydrated wet dunite or dry and hot olivine rheology. Both models display decoupled lithospheric layers leading to an eastward decrease of flexural rigidity from $\sim 10^{24}$ to $\sim 5 \cdot 10^{22}$ N m in Nepal and Bhutan, respectively.
Citation: Hammer, P., T. Berthet, G. Hetényi, R. Cattin, D. Drukpa, J. Chophel, S. Lechmann, N. Le Moigne, C. Champollion, and E. Doerflinger (2013), Flexure of the India plate underneath the Bhutan Himalaya, *Geophys. Res. Lett.*, *40*, 4225–4230, doi:10.1002/grl.50793.

1. Introduction

[2] The Himalayas stretch over 2400 km between the lowland of the Indian Shield and the highland of the Tibetan Plateau. At depth, the orogen marks the transition between regions of respectively regular and thickened crust. It is now well accepted that the shape of this transition is associated with regional isostasy that reflects the mechanical properties of the India plate bent beneath the mountain belt. Regional isostasy is well imaged and understood at the longitude of Kathmandu, where the upper mantle is the strongest layer of the lithosphere holding up the weight of both the Himalayas and the Tibetan Plateau [*Lyon-Caen and Molnar*, 1983; *Karner and Watts*, 1983; *Cattin et al.*, 2001; *Hetényi et al.*, 2006; *Nábělek et al.*, 2009].

[3] Although the tectonic units are remarkably uniform along the 2400 km long shape of the belt [*Schelling*, 1992; *Hodges*, 2000], there are hints of lateral heterogeneity. An east-west transition is indicated by different elevation profiles across the range [*Duncan et al.*, 2003], a reduction in crustal shortening [*McQuarrie et al.*, 2008; *Long et al.*, 2011], and patterns of focal mechanisms [*Hazarika et al.*, 2010]. At depth, although seismic tomography reveals spatial variation in the mantle structure [*Li et al.*, 2008], there is yet no image of the Moho's shape beneath the eastern Himalaya (east of Sikkim). Here following the approaches of *Lyon-Caen and Molnar* [1985], *Duroy et al.* [1989], and T. Berthet et al. (Lateral uniformity of India plate strength over Central and Eastern Nepal, submitted to *Geophysical Journal International*, 2013), we focus on variations between Nepal and the eastern Himalayas of Bhutan.

[4] After a brief presentation of the new gravity data collected in Bhutan, we discuss the obtained Bouguer anomaly profiles across the eastern Himalaya spanning from India to Tibet. Next, together with regional Moho depths available from seismology, we interpret this data set in terms of flexural rigidity using 2-D thermomechanical models simulating the bending and the rheology of the Indian lithosphere. Finally, from a comparison of the results to those in Nepal, we provide a first assessment of along-strike variations of flexural rigidity over the central and eastern Himalayas (Figure 1a).

2. Gravity Data

[5] Until now the Kingdom of Bhutan was a blank spot on the gravity data coverage map. To fill this data gap, we acquired new gravity data at 214 locations. Measurements were conducted with a *Scintrex CG5* relative gravimeter in 2010–2012 along all major roads in Bhutan.

[6] Following Berthet et al. (submitted manuscript, 2013), gravity measurements and dual-frequency GPS recordings are subjected to a standard processing scheme. The resulting Bouguer anomalies are computed using a reduction density of 2670 kg m^{-3} and include terrain corrections ranging from 5 to 80 mGal. The internally consistent but relative data set's accuracy is $\sim$3 mGal. Due to the lack of an absolute reference point, the data set is shifted to match the neighboring Bouguer anomalies in NE India and S Tibet. An error bar of $\pm$10 mGal is thus assigned to the new data set.

[7] Finally, these new Bouguer anomalies are combined with available Bouguer anomalies compiled by *Hetényi et al.* [2007] to construct continuous profiles across the Himalayan range, covering entirely the flexure of the India plate underneath the eastern Himalaya from the lowlands to the southern part of the Tibetan Plateau (Figure 1).

Additional supporting information may be found in the online version of this article.

[1]Department of Earth Sciences, ETH Zürich, Zurich, Switzerland.
[2]Géosciences Montpellier, Université Montpellier 2, Montpellier, France.
[3]Swiss Seismological Service, ETH Zürich, Zurich, Switzerland.
[4]Department of Geology and Mines, Ministry of Economic Affairs, Thimphu, Bhutan.

Corresponding author: G. Hetényi, Swiss Seismological Service, ETH Zürich, Sonneggstrasse 5, CH-8092 Zurich, Switzerland. (gyorgy.hetenyi@sed.ethz.ch)

0094-8276/13/10.1002/grl.50793

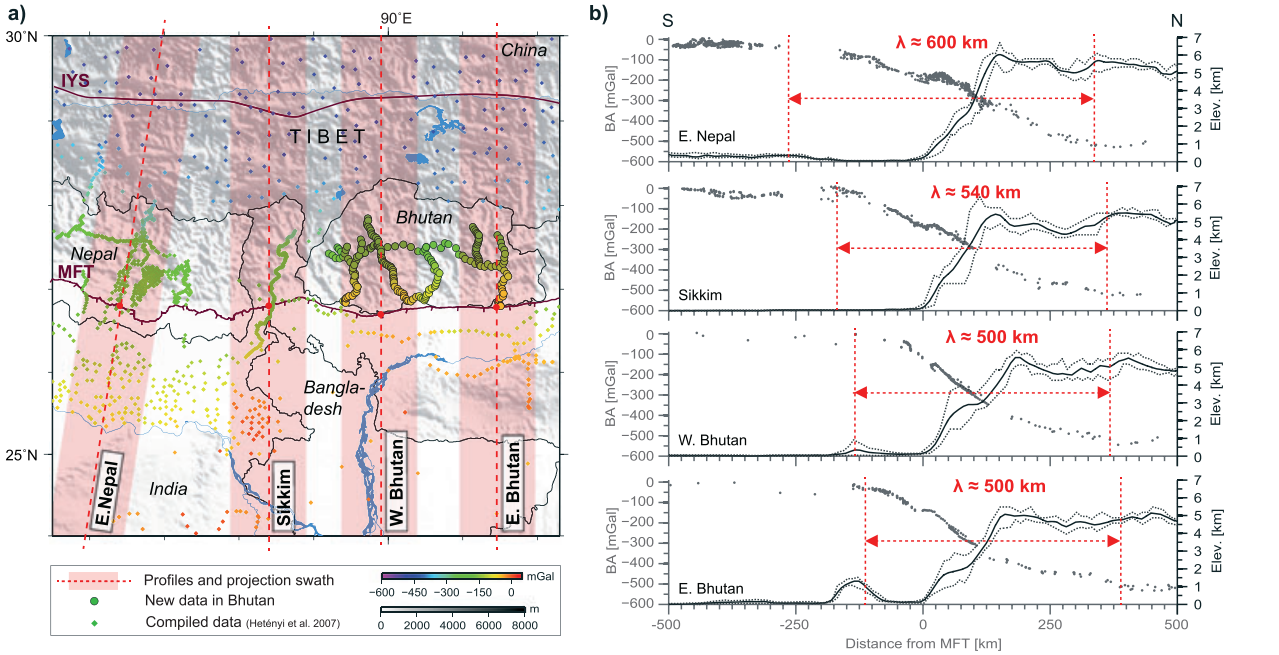

Figure 1. Map of the study area and projected Bouguer anomaly and topography profiles. (a) Map of E Nepal, Sikkim, and Bhutan with new and existing gravity data. Color scale is used for Bouguer anomaly. The center (red point) and orientation of the profiles, from W to E 26.8°N/86.4°N/8°, 26.8°N/88.4°E/0°, 26.7°N/89.9°E/0°, and 26.8°N/91.45°E/0°. Profile length ±500 km from center. Width of projected swaths ±50 km. Purple lines indicate the Indus-Yarlung Suture (IYS) and the Main Frontal Thrust (MFT). (b) Bouguer anomaly profiles (gray dots) and topography cross section (solid line: mean, dotted line: minimum and maximum topography in the projection swath). Red colors mark the characteristic wavelength of the flexure.

3. Bouguer Anomalies Across Bhutan

[8] Bouguer anomalies are projected along 1000 km long, arc-perpendicular profiles centered on the Main Frontal Thrust (MFT). Two profiles in E and W Bhutan are investigated and compared to profiles in E Nepal and in the Sikkim Himalaya to decipher along-strike variations (Figure 1b).

[9] Two distinct wavelengths can be identified on all profiles: The first-order anomaly is characterized by a long wavelength step function of ∼500 mGal over a distance of 500–600 km as measured between the kink points of approximately –50 to –20 mGal in the south in India and approximately –520 mGal in the north on the Tibetan Plateau. Hence, there is a roughly uniform northward gradient of –0.8 to –1.0 mGal km^{-1}, reflecting the increase in crustal thickness. Superimposed on this first-order anomaly is a second-order anomaly that defines an intermediate step near the MFT (0 km horizontal distance in Figure 1b).

[10] The first- and second-order anomalies exhibit along-strike variations between E Nepal and Bhutan. Most significant is a decrease in wavelength of the step function from west (∼600 km) to east (∼500 km) (Figure 1b). Lateral variation is further indicated by the level of the step superimposed on the linear gradient, shallowing west to east from –200 to –150 mGal. This is accompanied by an ∼100 km decrease of the distance between the southern kink point and the MFT. Hence, Bouguer anomalies in Bhutan start to decrease farther to the north relative to the position of the MFT, and the step near the MFT that is clearly observable in Nepal and Sikkim is narrower and of lower amplitude. The Sikkim profile represents a transition between those in Nepal and Bhutan from all perspectives (Figure 1b).

[11] These observed lateral changes in Bouguer anomalies are interpreted as the following:

[12] 1. The shorter distance between the kink points at the longitude of Bhutan is a clear indication of shorter wavelength lithosphere flexure with respect to that in Nepal.

[13] 2. In accordance with Bouguer anomaly profiles in Nepal [*Cattin et al.*, 2001; *Hetényi et al.*, 2006], where both seismic and borehole data constrain the geometry of the sedimentary basin, the step in the Bouguer anomalies near the MFT south of Bhutan is attributed to a low-density sedimentary infill of the foreland basin. The extent and depth of the foreland basin in the east (Brahmaputra) is however smaller than that in the central Himalayas (Ganges), as already pointed out by *Lyon-Caen and Molnar* [1983] and *Gansser* [1984] and shown in *Zhang* [1983].

4. Interpretation With Lithosphere Flexure Models

4.1. Thermomechanical Modeling

[14] To explore the implications of the shorter flexural wavelength on lithosphere rheology at the longitude of Bhutan, we take advantage of the finite element modeling tool *ADELI* [*Hassani et al.*, 1997]. This 2-D thermomechanical approach accounts for the viscoelastoplastic behavior of the lithosphere and its dependence on temperature and depth. The thermal structure of the underthrusting India plate is approximated by an analytical expression developed by *Royden* [1993]. A detailed description of the material laws and the thermal setup can be found in *Cattin et al.* [2001], *Hetényi et al.* [2006], and Berthet et al. (submitted

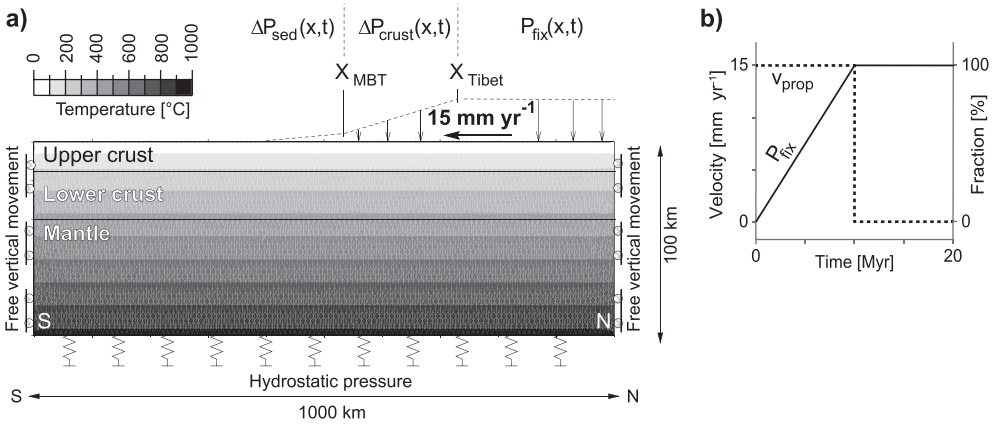

Figure 2. Setup of the thermomechanical model and time evolution of the load. (a) The load is composed of three spatial pressure regimes: a fixed load in Tibet $P_{\text{fix}}(x,t) = g(\rho_{\text{crust}}h_{\text{crust}} + \rho_{\text{topo}}h_{\text{topo}})$ and two variable loads that are recalculated after each time step to account for the changing thickness of the overlying Tibetan crust $\Delta P_{\text{crust}}(x,t) = g(\rho_{\text{crust}}h_{\text{crust}} + \rho_{\text{topo}}h_{\text{topo}})$ and of the foreland sediments $\Delta P_{\text{sed}}(x,t) = g\rho_{\text{sed}}h_{\text{sed}}$. Sedimentation in the Brahmaputra Basin is assumed to maintain a flat foreland at a constant zero elevation. The load is progressively moved to the south with an advance rate of 15 mm yr^{-1}. For isostatic balance, the model is supported by a hydrostatic pressure at its base. Free vertical displacements are allowed at the sides of the model. The upper crust, the lower crust, and the lithospheric mantle have different rheologies. The standard initial temperature distribution is shown. (b) Time evolution of the loads and of the propagation velocity v_{prop}.

manuscript, 2013), who successfully modeled the flexure of the India plate beneath Nepal using constraints from gravity and seismology.

[15] Following their approach, the initial geometry and density setup of the model was compiled using available controlled source as well as passive seismic results and velocity-density relations (Figure 2). During the simulations, the Indian lithosphere is bent down by the advancing (15 mm yr^{-1}) load of the Tibetan crust and sedimentation in the foreland basin. The Shillong Plateau south of the arc is not included in the model due to the poorly constrained time evolution and its unconstrained deep structure. A parametric study is performed assessing the influence of elastic, ductile, and thermal parameters on flexure wavelength. The nonuniqueness of the model is reduced by departing from a well-constrained model in central Nepal [*Cattin et al.*, 2001] and by developing two contrasting end-member models that define a parameter's space within which different combinations of setups likely lead to the same results (shape, flexural rigidity). Geometries produced by the model are evaluated by comparing synthetic and observed Bouguer anomalies and by crosschecking the flexural geometry with available regional seismic Moho constraints. Searching for the best fit models through 90 model simulations results in an evaluation of lithosphere rheologies of the India plate and produces two preferred models. Detailed information on the model setup, the range of values in the rheology parametric study, and the compilation of regional Moho constraints is presented in the supporting information.

4.2. Preferred Models

[16] The parametric study reveals that the creeping strength of the lithospheric mantle and the temperature field (controlled by the input temperature at the lithosphere-asthenosphere boundary (LAB)) are the two key factors that induce a shorter wavelength flexure. The ductile parameters of the crust as well as elastic material properties have a comparatively smaller influence.

[17] The two preferred models respectively use (1) a relatively weaker wet dunite rheology for the lithospheric mantle in a normal thermal regime (1000°C at the bottom of the model) and (2) a relatively stronger dry olivine rheology in a hotter (+150°C) thermal regime (see parameters in Table 1). Both of these models match the first- and second-order Bouguer anomaly variations and produce Moho depths coherent with the available seismological constraints. The shape of the intermediate step near the MFT is well fitted by a foreland basin of smaller extent and shallower depth compared to Nepal (Figure 3).

[18] Both preferred models induce a shorter wavelength flexure by altering the rheology of the lithospheric mantle compared to models developed for Nepal [*Cattin et al.*, 2001; *Hetényi et al.*, 2006]. Since the lithospheric mantle has a key role in supporting the weight of the Himalayas and the Tibetan Plateau, such lateral changes from the central to the eastern Himalaya therefore mark an important lithospheric boundary between the two regions.

[19] We note that a third type of model setup also produced an acceptable solution. In this setup, the southern edge of the Tibetan Plateau's load (an initial condition) was located 75 km farther to the south compared to other models, including those established for Nepal. Although

Table 1. Ductile Properties of the Two Best Fit Models[a]

	UC	LC	LM1	LM2
γ_0 (Pa^{-n} s^{-1})	$6.31 \cdot 10^{-25}$	$6.31 \cdot 10^{-20}$	$7.5 \cdot 10^{-17}$	$7 \cdot 10^{-14}$
n	2.9	3.05	3.3	3
E_a (kJ mol^{-1})	149	276	444	510

[a]The rheologies of the upper crust (UC) and of the lower crust (LC) are the same in the two best fit models. The wet dunite lithospheric mantle model (LM1) is run with a temperature at the LAB of Tm = 1000°C. The dry and hot olivine model (LM2) is run with Tm = 1150°C. Material laws used are described in *Cattin et al.* [2001] and *Hetényi et al.* [2006]. γ_0 and n are ductile power law parameters, and E_a is the activation energy. The following parameters were the same for all three layers: Young's modulus E = 50 GPa, Poisson's ratio ν = 0.25, cohesion c = 10 MPa, and internal friction angle ϕ = 30°.

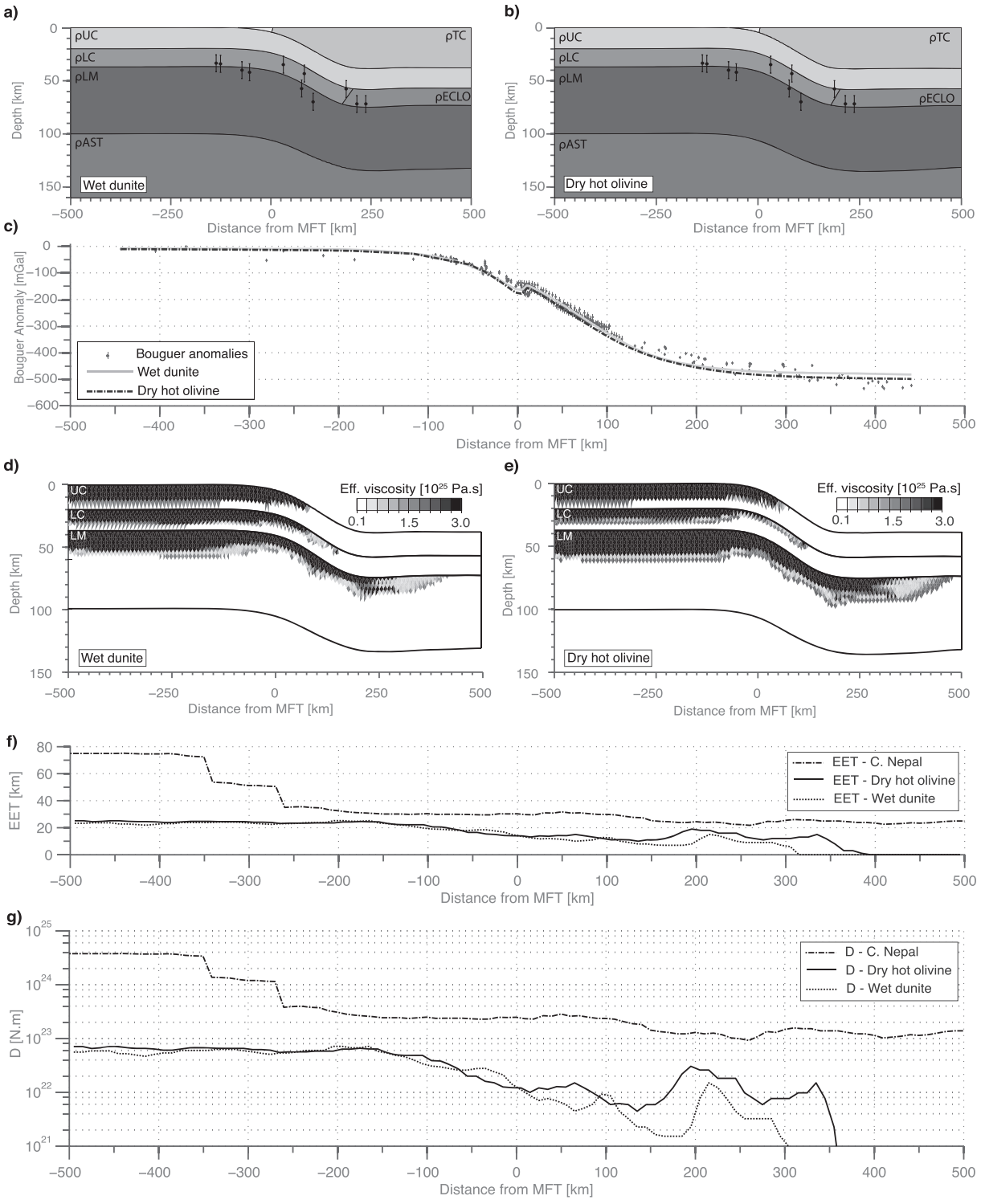

Figure 3. Preferred model results. (a, b) Resulting geometry with projected seismic Moho depths (dots with error bars) and density structure. Densities as in Table S1 and ρ_{ECLO} = 3050 kg m^{-3}. (c) Synthetic (lines) and observed Bouguer anomalies (dots with error bars). (d, e) Effective viscosity profiles. (f, g) Effective elastic thickness and flexural rigidity of the preferred models and of the Nepali model (Berthet et al., submitted manuscript, 2013) for comparison.

topography alone does not suggest such a difference with respect to Nepal, it is premature to confidently evaluate this model solution before accurate and high-resolution information on the Moho beneath Bhutan becomes available.

4.3. Flexural Strength of India

[20] The thermomechanical model provides information on the effective viscosity of the lithosphere. This is employed to assess the effective elastic thickness (EET) of the lithosphere, which is the thickness of an elastic plate having an equivalent flexural rigidity to that of the layered viscoelastoplastic plate. This calculation is performed by taking the cubic average of lithospheric layer's elastic core thickness [*Burov and Diament*, 1995]. We use a threshold value of $1.6 \cdot 10^{25}$ Pa s for the deformation to be considered elastic, which is equivalent to assuming a characteristic viscous relaxation time of 10 Myr for a Young's modulus of 50 GPa.

[21] The EET estimates of both preferred model types reflect the northward decrease in strength of the lithosphere in response to thermal and flexural weakening under the high range and the foreland basin (Figure 3). The individual elastic cores are decoupled all along the profile which results in a relatively low EET even beneath India. Here the maximum values of 25 km are reached, which are significantly less than those in Central Nepal. There the lithospheric layers are coupled on the southern part of the profile yielding EET values reaching 75 km and still at 40 km where the lithosphere layers decouple (Berthet et al., submitted manuscript, 2013). Since these EET values were calculated with a slightly different Young's modulus (and therefore threshold viscosity values), a comprehensive comparison can be made using flexural rigidity D [*Burov and Diament*, 1995]:

$$D = \frac{E \cdot \mathrm{EET}^3}{12(1-\nu^2)} \tag{1}$$

where ν is the Poisson's ratio (0.25) and E is the respective Young's modulus. Flexural rigidity of the India plate south of Bhutan is $6.9 \cdot 10^{22}$ N m at most, while it is $3.8 \cdot 10^{24}$ N m south of Nepal where the lithosphere layers are coupled and $5.7 \cdot 10^{23}$ N m as they decouple south of the MFT. Reconverting these values to EET with the parameters used in this study yields 25 (Bhutan), 94 (Nepal, coupled), and 50 km (Nepal, decoupled), pointing to a significant along-strike difference in flexural strength.

[22] The west-to-east decrease of flexural rigidity (and consequently of EET) from the central to the eastern Himalaya is in agreement with the findings of *Jordan and Watts* [2005] and extends those of *Bilham et al.* [2003]. Finally, both our model solutions for the India plate beneath Bhutan presented here clearly confirm the findings for central Nepal regarding the key role of the uppermost mantle, which remains the strongest layer of the lithosphere.

5. Conclusions

[23] New gravity data in Bhutan provide the first constraints on the flexural geometry of the Indian lithosphere underneath this part of the Himalayas. Compared to Nepal, the lithosphere bends down over a shorter distance.

[24] An extensive set of numerical simulations of rheology parameters yields two alternative model types that explain the available geophysical data, including gravity and seismological measurements. Compared to Nepal, both models lower the ductile strength of the lithospheric mantle: one suggests hydration (wet dunite rheology), the other elevated temperature at the base of the lithosphere (hot dry olivine rheology).

[25] The associated effective elastic thickness estimates, displaying a relatively low maximum value (25 km) and a general northward decrease due to thermal and flexural weakening, point to decoupled lithospheric layers. Still, the strongest layer is the uppermost mantle holding up the weight of the orogen, thus demonstrating its main role in continental lithosphere strength.

[26] **Acknowledgments.** The authors would like to thank all people helping in realizing the field measurements across Bhutan: officials, drivers, and people of the countryside. We are grateful to E. Kissling for advice and discussion during the ETH Master Thesis from which this paper resulted. We are also thankful for the constructive comments by P. Molnar and two anonymous reviewers. We are indebted for the seed funding granted by the North-South Centre and ETH Zürich.

[27] The Editor thanks Djordje Grujic for assistance in evaluating this paper.

References

Bilham, R., R. Bendick, and K. Wallace (2003), Flexure of the Indian plate and intraplate earthquakes, *Proc. Indian Acad. Sci. (Earth Planet. Sci.)*, *112*, 315–329.

Burov, E. B., and M. Diament (1995), The effective elastic thickness (T_e) of continental lithosphere—What does it really mean? *J. Geophys. Res.*, *100*, 3905–3927, doi:10.1029/94JB02770.

Cattin, R., G. Martelet, P. Henry, J. P. Avouac, M. Diament, and T. R. Shakya (2001), Gravity anomalies, crustal structure and thermomechanical support of the Himalaya of central Nepal, *Geophys. J. Int.*, *147*, 381–392.

Duncan, C., J. Masek, and E. Fielding (2003), How steep are the Himalaya? Characteristics and implications of along-strike topographic variations, *Geology*, *31*, 75–78.

Duroy, Y., A. Farah, and R. J. Lillie (1989), Subsurface densities and lithospheric flexure of the Himalayan foreland in Pakistan, *Spec. Pap. Geol. Soc.*, *232*, 217–236.

Gansser, A. (1984), Facts and theories on the Himalayas, *Eclogae Geol. Helv.*, *84*, 33–59.

Hassani, R., D. Jongmans, and J. Chery (1997), Study of plate deformation and stress in subduction processes using two-dimensional numerical models, *J. Geophys. Res.*, *102*, 17,951–17,965, doi:10.1029/97JB01354.

Hazarika, P., M. R. Kumar, G. Srijayanthi, P. S. Raju, N. P. Rao, and D. Srinagesh (2010), Transverse tectonics in the Sikkim Himalaya: Evidence from seismicity and focal mechanism data, *Bull. Seismol. Soc. Am.*, *100*(4), 1816–1822, doi:10.1785/0120090339.

Hetényi, G., R. Cattin, J. Vergne, and J. L. Nábělek (2006), The effective elastic thickness of the India Plate from receiver function imaging, gravity anomalies and thermomechanical modelling, *Geophys. J. Int.*, *167*, 1106–1118, doi:10.1111/j.1365-246X.2006.03198.x.

Hetényi, G., R. Cattin, F. Brunet, L. Bollinger, J. Vergne, J. Nábělek, and M. Diament (2007), Density distribution of the India plate beneath the Tibetan Plateau: Geophysical and petrological constraints on the kinetics of lower-crustal eclogitization, *Earth Planet. Sci. Lett.*, *264*(1), 226–244, doi:10.1016/j.epsl.2007.09.036.

Hodges, K. V. (2000), Tectonics of the Himalaya and southern Tibet from two perspectives, *Geol. Soc. Am. Bull.*, *112*, 324–350.

Jordan, T. A., and A. B. Watts (2005), Gravity anomalies, flexure and the elastic thickness structure of the India-Eurasia collisional system, *Earth Planet. Sci. Lett.*, *236*, 732–750, doi:10.1016/j.epsl.2005.05.036.

Karner, G. D., and T. Watts (1983), Gravity anomalies and flexure of the lithosphere at mountain ranges, *J. Geophys. Res.*, *88*, 10,449–10,477.

Li, C., R. D. Van der Hilst, A. S. Meltzer, and E. R. Engdahl (2008), Subduction of the Indian lithosphere beneath the Tibetan Plateau and Burma, *Earth Planet. Sci. Lett.*, *274*(1-2), 157–168, doi:10.1016/j.epsl.2008.07.016.

Long, S., N. McQuarrie, T. Tobgay, and D. Grujic (2011), Geometry and crustal shortening of the Himalayan fold-thrust belt, eastern and central Bhutan, *Geol. Soc. Am. Bull.*, *123*(7-8), 1427–U244, doi:10.1130/B30203.1.

Lyon-Caen, H., and P. Molnar (1983), Constraints on the structure of the Himalaya from an analysis of gravity-anomalies and a flexural model of the lithosphere, *J. Geophys. Res.*, *88*, 8171–8191, doi:10.1029/JB088iB10p08171.

Lyon-Caen, H., and P. Molnar (1985), Gravity anomalies, flexure of the Indian plate, and the structure of the Himalaya and Ganga basin, *Tectonics*, *4*, 513–538.

McQuarrie, N., D. Robinson, S. Long, T. Tobgay, D. Grujic, G. Gehrels, and M. Ducea (2008), Preliminary stratigraphic and structural architecture of Bhutan: Implications for the along-strike architecture of the Himalayan system, *Earth Planet. Sci. Lett.*, *272*(1-2), 105–117, doi:10.1016/j.epsl.2008.04.030.

Nábělek, J., G. Hetényi, J. Vergne, S. Sapkota, B. Kafle, M. Jiang, H. P. Su, J. Chen, and B. S. Huang (2009), Underplating in the Himalaya-Tibet collision zone revealed by the Hi-CLIMB experiment, *Science*, *325*, 1371–1374.

Royden, L. H. (1993), The steady state thermal structure of eroding orogenic belts and accretionary prisms, *J. Geophys. Res.*, *98*, 4487–4507, doi:10.1029/92JB01954.

Schelling, D. (1992), The tectonostratigraphy and structure of the eastern Nepal Himalaya, *Tectonics*, *11*, 925–943, doi:10.1029/92TC00213.

Zhang, W. (1983), *The Marine and Continental Tectonic Map of China and Its Environs 1:5,000,000*, Science Press, Beijing, China.